Vol. 7 • No. 2 • January 22 • 2020

ADVANCED SCIENCE

Open Access

WILEY-VCH

www.advancedscience.com

ADVANCED SCIENCE Open Access
www.advancedscience.com

DNA-Mediated Assembly of Multispecific Antibodies for T Cell Engaging and Tumor Killing

*Liqiang Pan, Chan Cao, Changqing Run, Liujuan Zhou, and James J. Chou**

Targeting T-cells against cancer cells is a direct means of treating cancer, and has already shown great responses in clinical treatment of B-cell malignancies. A simple way to redirect T-cells to cancer cells is by using multispecific antibody (MsAb) that contains different arms for specifically "grabbing" the T-cells and cancer cells; as such, the T-cells are activated upon target engagement and the killing begins. Here, a nucleic acid mediated protein–protein assembly (NAPPA) approach is implemented to construct a MsAb for T-cell engaging and tumor killing. Anti -CD19 and -CD3 single-chain variable fragments (scFvs) are conjugated to different L-DNAs with sequences that form the Holliday junction, thus allowing spontaneous assembly of homogeneous protein–DNA oligomers containing two anti-CD19 and one anti-CD3 scFvs. The new MsAb shows strong efficacy in inducing Raji tumor cell cytotoxicity in the presence of T-cells with $EC_{50} \approx 0.2 \times 10^{-9}$ M; it also suppresses tumor growth in a Raji xenograft mouse model. The data indicates that MsAbs assembled from protein–DNA conjugates are effective macromolecules for directing T-cells for tumor killing. The modular nature of the NAPPA platform allows rapid generation of complex MsAbs from simple antibody fragments, while offering a general solution for preparing antibodies with high-order specificity.

1. Introduction

The essence of bispecific antibody (BsAb) is that two different antigen binding domains are physically linked such that they can engage multiple cells presenting different antigens, and many creative methods have been developed to achieve this property.[1,2] In many of the early proof-of-concept studies, BsAbs were generated by chemically crosslinking two different IgGs or Fabs using bifunctional crosslinking reagents that react specifically with the thiol and primary amine groups of the antibody.[3,4] Although several of BsAbs prepared in this way have advanced to clinical trials,[5–7] large majority of BsAbs currently being developed are generated with recombinant antibody engineering. Over 100 different formats of multispecific antibodies (MsAbs) have been engineered based on the immunoglobulin G (IgG) or its components (reviewed in ref. [1]), some containing the Fc and others do not. Well-known examples of Fc-less formats are tandem single-chain variable fragments (scFvs)[8] and tandem nanobodies.[9] Among them, the bispecific T-cell engager (BiTE) consisting of tandem anti-CD19 and anti-CD3 scFvs (blinatumomab) is the first FDA approved BsAb, used for treating acute lymphoblastic leukemia.[10,11] Natural IgG containing the Fc is symmetric. To introduce bispecific or asymmetric property to the IgG, a variety of methods have been developed to favor heterodimeric heavy chain pairing. A few prominent examples are knob-into-hole,[12] structural-based mutagenesis,[13] and electrostatic steering[14] that favors heterodimerization or disfavors homodimerization of the Fc. Further, combining the knob-into-hole and appending one of the two arms of the IgG with another scFv or Fab allows the assembly of trispecific antibody.[15]

The above are only a few examples of BsAb engineering. The fact that many of the BsAbs with different sizes and forms all showed strong ability to mediate T-cell engaging suggests that if the antibody domains targeting different antigens stay intact within a molecular framework, the form of the framework may not be so important as long as it does not place the antigen-recognition domains too far apart. Inspired by the previous works, we implemented the nucleic acid mediated protein–protein assembly method,[16–18] designated NAPPA here, to construct a MsAb to drive T-cell—tumor cell engagement and tested the in vitro and in vivo efficacy of the new molecular complex.

2. Results

In our NAPPA implementation (illustrated in **Figure 1**), scFvs targeting different antigens each were chemically conjugated,

Dr. L. Pan
Institute of Drug Metabolism and Pharmaceutical Analysis and Zhejiang Province Key Laboratory of Anti-cancer Drug Research
College of Pharmaceutical Sciences
Zhejiang University
310058 Hangzhou, China
Dr. C. Cao, Dr. C. Run, L. Zhou
Assembly Medicine, LLC
Shanghai 201203, China
Dr. J. J. Chou
Department of Biological Chemistry and Molecular Pharmacology
Harvard Medical School
Boston, MA 02115, USA
E-mail: james_chou@hms.harvard.edu
The ORCID identification number(s) for the author(s) of this article can be found under https://doi.org/10.1002/advs.201900973.

DOI: 10.1002/advs.201900973

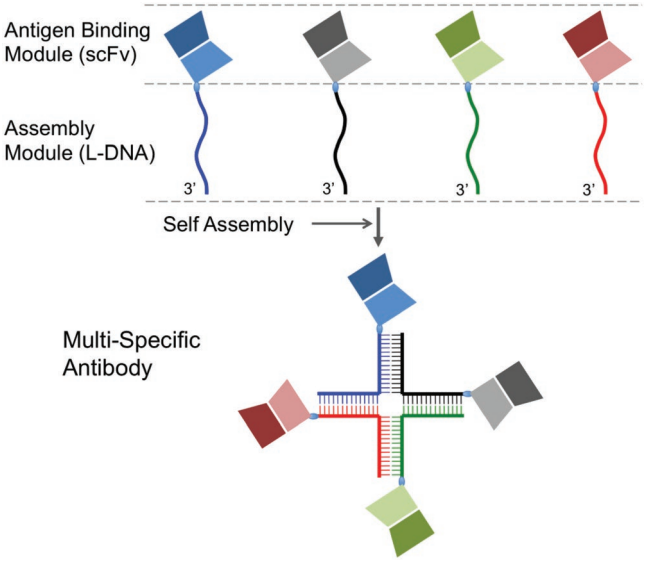

Figure 1. Schematic illustration of the NAPPA implementation for generating multispecific antibodies.

at their C-termini, to a 30-base DNA that was designed to pair with DNAs linked to other scFvs, and the scFv-DNA conjugates were purified separately. Hence, in this format, the scFvs are the antigen binding modules (ABMs) and DNAs are the assembly modules. We could then assemble the multispecific scFv oligomer by simply mixing the pre -purified and -stored scFv-DNAs at the designated molar ratio. Owing to the accuracy of DNA base pairing interaction, the spontaneously assembled scFv-DNA oligomers should be homogeneous, stable, and readily usable in T-cell engaging experiments.[17]

Several specific details of the above implementation are important for the therapeutic applicability of the final assembled product. First, the DNAs should be synthesized as left-handed DNAs (L-DNAs) to prevent degradation by nucleases in vivo. L-DNAs are not substrates of any of the known enzymes in nature while still being able to form base-pairing interactions as D-DNAs.[19,20] Moreover, the L-form nucleic acids are nonimmunogenic, as was demonstrated for several L-form aptamers (spiegelmers) that have advanced to clinical trials.[21] Second, the DNA is conjugated to the C-terminus of the scFv so that it is less likely to interfere with the complementarity-determining regions (CDRs). Finally, the length of DNAs should be set such that the melting temperature (T_m) of each of the paired double-stranded segments is greater than 50 °C, to ensure the stability of the oligomeric complex. Based on the above considerations, we constructed a MsAb containing two anti-CD19 scFvs ($scFv^{CD19}$) and one anti-CD3 scFv ($scFv^{CD3}$), gathered in a DNA four-way junction complex (**Figure 2**a), designated NAPPA001.

The sequence of the $scFv^{CD19}$ was taken from the CD19-CD3 bispecific antibody Blincyto, which is the first FDA-approved BsAb for use in cancer immunotherapy.[10] The $scFv^{CD3}$ sequence used here is from the anti-CD3 mAb OKT3.[22] The scFvs, all containing a free cysteine at the C-terminus (scFv-C) for DNA conjugation, were expressed in *Escherichia coli* as a C-terminal fusion component to the polyhistidine-tagged maltose binding protein (H_6-MBP). A TEV cleavage site was inserted between MBP and scFv for separation of the two during purification. The purification of the scFv-DNA conjugates was straightforward (details described in Supporting Information). Briefly, the H_6-MBP-scFv-C was purified using amylose affinity and treated with TEV enzyme to release strep tagged-scFv-C (scFv-C). The scFv-C was purified by size exclusion chromatography, followed by conjugation to L-DNA at its C-terminal Cys (Figure 2b). For chemical conjugation, the 5′ end of the L-DNA was first linked to the PEGylated SMCC bifunctional linker via a reaction of a primary amine on the L-DNA with the NHS ester of the linker. The purified SMCC-PEG2-L-DNA was then linked to the scFv-C via a reaction of the SMCC maleimide with the free thiol of the fusion protein. The reaction mixture was then subject to Strep-Tactin affinity chromatography for removing free DNA. In the final step, ion-exchange chromatography was used to remove proteins not conjugated to DNA, yielding pure scFv-L-DNA. Reducing agent (10×10^{-6} M TCEP) was used throughout all purification steps before conjugation reaction to keep the C-terminal free Cys reduced.

Following the above protocol, we prepared three scFv-L-DNAs: two $scFv^{CD19}$ linked to DNAs 1 and 2, respectively, and one $scFv^{CD3}$ linked to DNA4 (DNA sequences shown in Figure 2a). The final MsAb, designated NAPPA001, was assembled by mixing equal moles of $scFv^{CD19}$-L-DNA1, $scFv^{CD19}$-L-DNA2, L-DNA3, and $scFv^{CD3}$-L-DNA4 (Figure 2c). Nuclease digestion tests showed that the assembled L-DNA tetramer was completely resistant to DNAse I, T7 endonuclease, S1 nuclease, and Exonuclease I, whereas that assembled with corresponding D-DNAs was degraded rapidly (Figure 2d). We have also shown that the assembled L-DNA tetramer is stable in fetal bovine serum (Figure S1, Supporting Information).

We next tested the ability of the scFv-L-DNA oligomer to engage T-cells against the Raji cells, which are B-lymphocytes that express CD19 on the cell surface. The CD3-expressing T-cells were from human peripheral blood mononuclear cell (hPBMC). The $(scFv^{CD19})_2$-$scFv^{CD3}$ has two ABMs to interact with the Raji cell CD19s and one ABM to interact with the T-cell CD3. Engaging the two cells should activate the T-cells, leading to the formation of immunological synapses with the Raji cells and their eventual lysis. In this experiment, we used [Effector T-cell]:[Tumor cell] (E:T) ratio of 10:1, and examined tumor lysis and T-cell activation induced by various doses of the new MsAb. For tumor lysis, we used lactate dehydrogenase (LDH) detection kit to quantify LDH release from dead cells with impaired membrane integrity. To quantitate T-cell activation, we measured the expression level of CD25 or CD137 (4-1BB) on $CD3^+$ cells by flow cytometry analysis of CD25/CD3 or CD137/CD3 coimmunostaining, respectively. The in vitro assay showed favorable efficacy of NAPPA001 in inducing tumor cell lysis (**Figure 3**a). Although NAPPA001 was generated from two scFvs with relatively low affinity ($K_D \approx 10^{-7}$ M) (Figure S2, Supporting Information), it showed powerful target cell killing with a EC_{50} of $\approx 0.2 \times 10^{-9}$ M after two days of incubation. Independent control experiments have been performed to address the possibility that multivalent antibody binding alone can be toxic to lymphoma cells.[23] These experiments showed that 1) the NAPPA001 does not induce Raji cell lysis in the absence of hPBMC (Figure S3, Supporting Information), 2) the unassembled $scFv^{CD19}$ and $scFv^{CD3}$ in the absence or presence of L-DNA Holliday junction

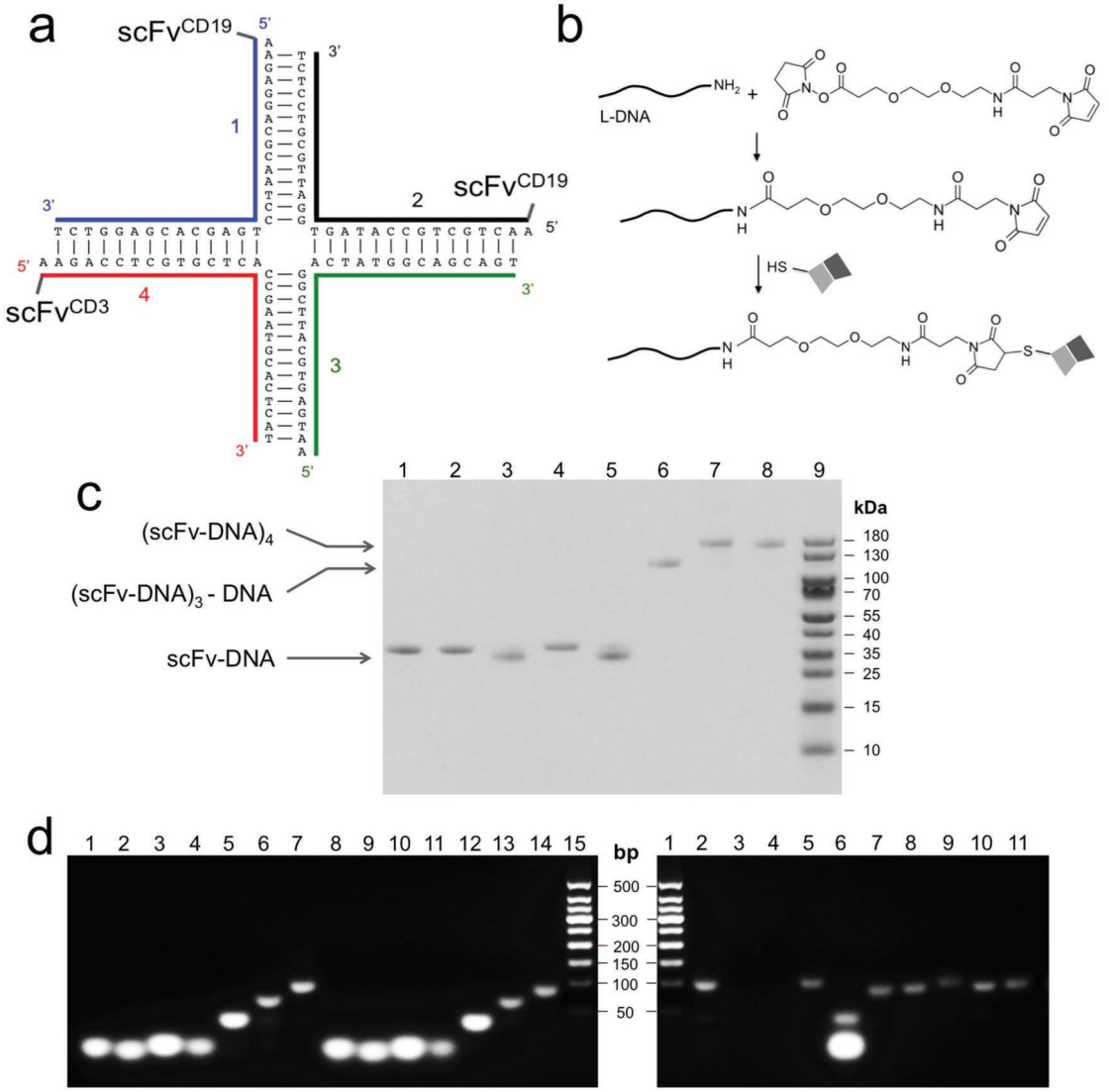

Figure 2. Preparation of the $(scFv^{CD19})_2$-$scFv^{CD3}$ antibody using the NAPPA method. a) Sequences of four DNAs that form the 4-way junction and the conjugation of scFv to three of the four DNAs. b) Reaction scheme for linking L-DNA to the scFv-C via PEGylated SMCC. c) SDS-PAGE analysis of various assemblies of scFv-L-DNA conjugates. Lane definitions are: 1—$scFv^{CD19}$-L-DNA1; 2—$scFv^{CD19}$-L-DNA2; 3—$scFv^{CD3}$-L-DNA3; 4—$scFv^{4\text{-}1BB}$-L-DNA4; 5—$scFv^{CD3}$-L-DNA4; 6—$scFv^{CD19}$-L-DNA1 + $scFv^{CD19}$-L-DNA2 + L-DNA3 + $scFv^{CD3}$-L-DNA4; 7—$scFv^{CD19}$-L-DNA1 + $scFv^{CD19}$-L-DNA2 + $scFv^{CD3}$-L-DNA3 + $scFv^{CD3}$-L-DNA4; 8—$scFv^{CD19}$-L-DNA1 + $scFv^{CD19}$-L-DNA2 + $scFv^{4\text{-}1BB}$-L-DNA3 + $scFv^{CD3}$-L-DNA4; 9—MW marker. d) Agarose gel electrophoresis analysis of L-DNA assemblies and resistance to nucleases. Lanes in the left gel: 1—D-DNA1; 2—D-DNA2; 3—D-DNA3; 4—D-DNA4; 5—D-DNAs 1, 2; 6—D-DNAs 1–3; 7—D-DNAs 1–4; 8–14—same as 1–7 but for L-DNAs; 15—molecular weight (MW) marker. Lanes in the right gel: 1—MW marker; 2—assembled D-DNA tetramer (1–4); 3–6—D-DNA tetramer with added DNAase, S1, Exol, and T7 nucleases, respectively; 7—L-DNA tetramer (1–4); 8–11—same as in 3–6 but for L-DNA tetramer.

also do not induce significant cytotoxicity in the presence of hPBMC (Figure S3, Supporting Information), and 3) $scFv^{CD19}$-$scFv^{CD3}$ BsAb assembled with L-DNA duplex can induce Raji cell lysis in the presence of hPBMC (Figure S3, Supporting Information), thus confirming that the cytotoxicity was due to T-cell redirecting mediated specifically by the MsAb. In another experiment, the T-cells were activated by the presence of 10×10^{-12} M NAPPA001 according to the increased expression level of CD25, a biomarker for late stage T-cell activation (Figure 3b). Further, cell surface expression of the costimulatory receptor 4-1BB was upregulated by the MsAb treatment (Figure 3b), giving rise to the possibility of further leveraging T-cell activity through simultaneous activation of 4-1BB with our flexible MsAb platform.

A similar scFv-L-DNA oligomer was constructed to engage T-cells against the CEA^+ LS174T cells, which is a model cell line for solid tumor—human colorectal adenocarcinoma. In this case, the NAPPA001 (Figure 2a) was modified to specifically target CEA (carcinoembryonic antigen) by replacing the two anti-CD19 scFvs with two anti-CEA scFvs, derived from PR1A3 (a mouse anti-human CEA antibody).[24] Using the same E:T ratio of 10:1, the new MsAb, $(scFv^{CEA})_2$-$scFv^{CD3}$ (designated NAPPA002) showed target cell killing with EC_{50} of $\approx 1.0 \times 10^{-9}$ M after two days of incubation (Figure 3c).

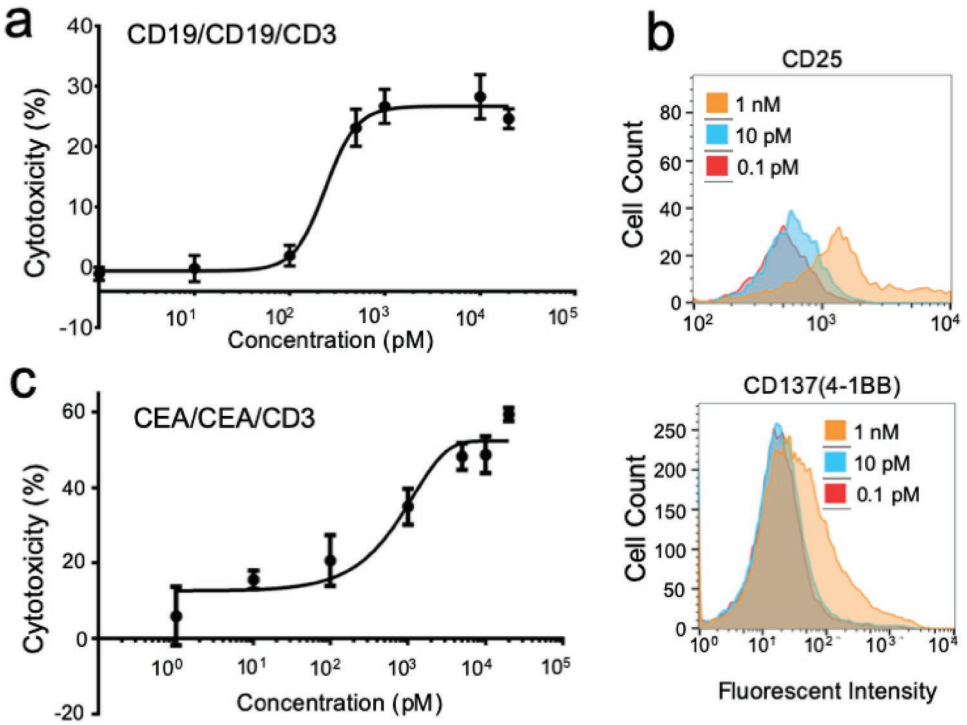

Figure 3. T-cell redirecting function of $(scFv^{CD19})_2$-$scFv^{CD3}$ and $(scFv^{CEA})_2$-$scFv^{CD3}$. a) Effect of treating $CD19^+$ Raji cells with NAPPA001 (at various concentration) and hPBMC (E:T ratio 10:1). Cell viability was measured using the LDH detection kit after 2 days of incubation in 96-well plate. Cytotoxicity (%) was calculated as [sample LDH release—background LDH release]/[maximum LDH release—background LDH release] × 100, where background LDH release is from Raji cells incubated with hPBMC without MsAbs and maximum LDH release is from Raji cells treated with 1% Triton X-100. b) Expression levels of CD25 (left) and CD137 (right) on hPBMC cell surface induced by NAPPA001 in the presence of the Raji cells. hPBMC and Raji cells were mixed at E:T ratio of 10:1, followed by the addition of 0.1×10^{-12}, 10×10^{-12}, or 1×10^{-9} M of NAPPA001. After 2-day incubation, cells were coimmunostained with anti-CD25 and anti-CD3 antibodies (for detecting CD25 expression on T-cell surface) or anti-CD137 and anti-CD3 antibodies (for detecting CD137 expression), and examined by flow cytometry. c) Effect of treating CEA^+ LS174T cells with NAPPA002 (see text) and hPBMC (E:T ratio 10:1). Cell viability was measured as described above.

To test whether the scFv-L-DNA complex can be absorbed into animal bloodstream and distributed to the tumor sites via the circulatory system, we examined its antitumor activity in mice in a subcutaneous $CD19^+$ Raji xenograft model. In this study, the cultured Raji cells were cografted with hPBMC at E:T ratio of 4:1. Mixed cells were injected subcutaneously into immunodeficient NSG mice. The $(scFv^{CD19})_2$-$scFv^{CD3}$ (given at 10 μg per mouse) or vehicle (phosphate-buffered saline (PBS)) was administered intravenously twice per week for four weeks starting 3 days after tumor/hPBMC cografting. The results

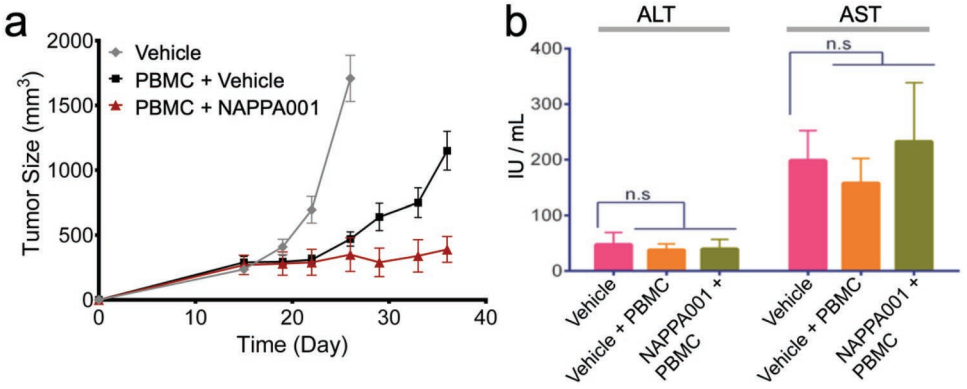

Figure 4. In vivo efficacy and toxicity of NAPPA001 in human Burkitt's lymphoma xenograft mouse model. a) In vivo efficacy of NAPPA001 in human Burkitt's lymphoma xenograft mouse model. Raji tumor cells were implanted or coimplanted with human PBMC (E:T ratio is 4:1) subcutaneously into NSG mice ($n = 5$) and treated with either PBS (vehicle) in the absence (gray) or presence (black) of PBMC, or PBMC with NAPPA001 (10 μg per mouse) (red) via intravenous injection twice a week starting 3 days after Raji/PBMC cografting for 4 weeks. b) Serologic examination of potential hepatotoxicity of NAPPA001. Serum samples were collected from each group 24 h after the fourth injection of NAPPA001. AST and ALT levels were examined by ELISA in two duplicates, and mean value was calculated from AST and ALT levels in five mice in each group ($n = 5$).

indicate that mice treated with NAPPA001 almost completely suppressed tumor growth until the end of the study (37 days), in contrast to the rapid tumor growth in the control group (treated with PBS) (**Figure 4**a). Serological examination of the NAPPA001-treated group showed no abnormal levels of aspartate aminotransferase (AST) and alanine aminotransferase (ALT) in comparison to the vehicle group, suggesting the MsAb posed no detectable hepatoxicity (Figure 4b). Steady increase of mice body weight further excluded any severe MsAbs-related global toxicity (Figure S4, Supporting Information).

NAPPA002 ($(scFv^{CEA})_2$-$scFv^{CD3}$) was also tested for efficacy in mice using a similar protocol. In this case, CEA^+ LS174T cells were cografted with hPBMC at E:T ratio of 5:1, and NAPPA002 (given at 20 µg per mouse) or vehicle (PBS) was administered intravenously twice per week starting 3 days from cografting for 1.5 weeks. The results show that mice treated with NAPPA002 also significantly suppressed the solid tumor growth compared with the vehicle control groups (Figure S5, Supporting Information).

We further examined the property of the LS174T-targeting MsAb in targeting and infiltrating solid tumors in vivo. For this experiment, we constructed a fluorescent version of NAPPA002 by conjugating the fluorescent probe NHS-Cy5.5 to the 5′ end of L-DNA3 (see Figure 2a). The resulting MsAb, $(scFv^{CEA})_2$-$scFv^{CD3}$-Cy5.5, was tested in the LS174T xenograft mouse model. After the implanted tumor (in the right flank of mice) reached ≈500 mm^3, $(scFv^{CEA})_2$-$scFv^{CD3}$-Cy5.5 or PBS (vehicle) was injected intravenously and the mice were imaged at different time points. We found that $(scFv^{CEA})_2$-$scFv^{CD3}$-Cy5.5 rapidly reached the tumor and penetrated into it within one hour, and continued to accumulate at the tumor site, while randomly distributed MsAbs were gradually metabolized (**Figure 5**a). The tumor site was accompanied by strong fluorescence from different directions (ventral and lateral), indicating colocalization of tumor and $(scFv^{CEA})_2$-$scFv^{CD3}$-Cy5.5. This result confirmed the ability of the new MsAbs to infiltrate solid tumors. The half-life of $(scFv^{CEA})_2$-$scFv^{CD3}$-Cy5.5 was calculated by fluorescence quantification to be ≈16 h (Figure 5b).

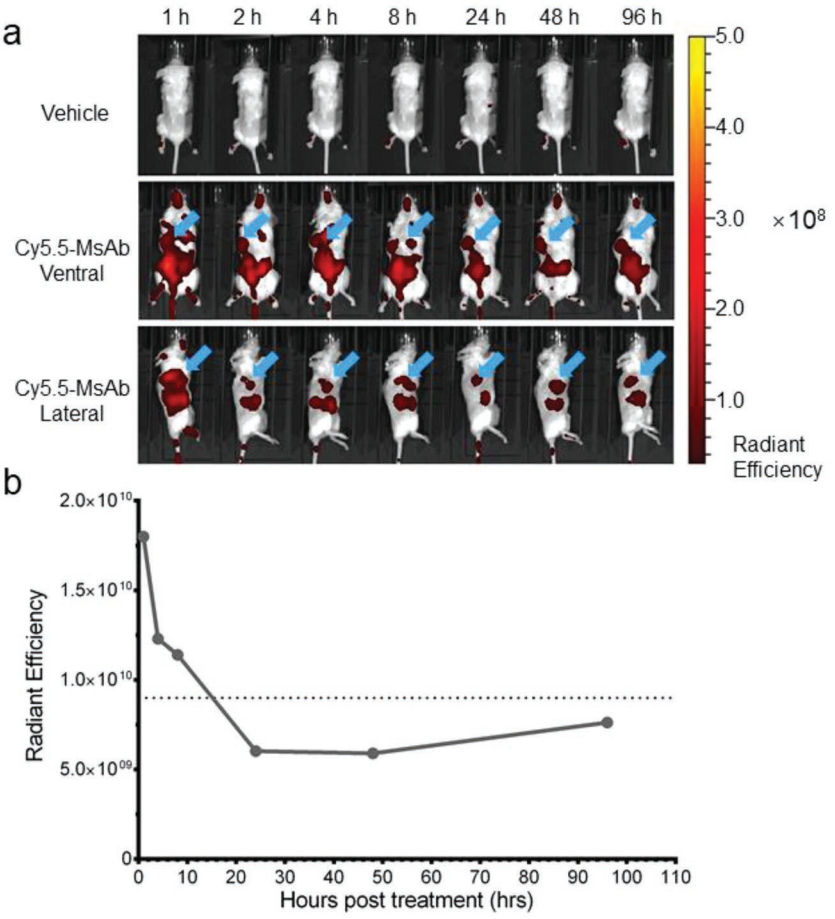

Figure 5. In vivo distribution and pharmacokinetics of $(scFv^{CEA})_2$-$scFv^{CD3}$-Cy5.5 in LS174T xenograft mouse model. a) Fluorescent images of mice with LS174T and PBMCs (mixed at E:T ratio of 5:1) implanted subcutaneously into the right flanks, injected intravenously with PBS (vehicle) or 100 µg of $(scFv^{CEA})_2$-$scFv^{CD3}$-Cy5.5 after the solid tumor reached 500 mm^3. The fluorescence in mice were monitored and quantified by a small animal imager (PerkinElmer IVIS Kinetic III) at different time points. Fluorescence is represented graphically as radiant efficiency (photons s^{-1} cm^{-2} per str)/(µW cm^{-2}). Blue arrows indicate the position of the implanted tumor. b) Plot of fluorescence intensity at different time points after injection of the fluorescent MsAb, showing that the half-life of the MsAb is ≈16 h.

3. Discussion

We have shown that multiple scFvs targeting different antigens, linked together by a L-DNA scaffold, is a stable molecular complex that can efficiently induce T-cell—tumor cell engagement in vitro and in vivo. We believe the NAPPA format should have little to no toxicity or immunogenicity in vivo. Comparing with other MsAb formats, the major addition of NAPPA is the linker-L-DNA. The L-form nucleic acids are nonimmunogenic and generally not toxic, since they have advanced to clinical trials.[21] The PEG spacer within the PEGylated SMCC linker should have the effect of enhancing stability and reducing aggregation and immunogenicity.[25,26] The SMCC linker is widely used in preparing antibody drug conjugate (ADC). For example, in the case of the Trastuzumab-SMCC-DM1 ADC that targets HER2, no SMCC-associated immunogenicity or toxicity was reported in clinical trials.[27]

Probably the biggest advantage of the NAPPA method is that it allows the option to prepare and store individual scFv-L-DNA conjugates separately, each targeting one of the known tumor antigens or immune cell activators, and then assemble a prescribed combination of them into MsAb immediately before use. This type of flexibility would be compatible with personalized cancer immunotherapy, as tumor antigen expression can

vary substantially among patients. We found that when the concentrations of the scFv-L-DNA conjugates were determined accurately, mixing them at equal molar ratio could generate very homogeneous oligomeric specie.

Another notable advantage is that multistrand DNA assembly affords unlimited possibilities and one of them is achieving higher order oligomers. We used four complementary DNA strands to generate a BsAb containing three scFvs (two anti-CD19 and one anti-CD3). In this case, two DNA strands carried the same $scFv^{CD19}$, the third did not carry anything, and the fourth carried $scFv^{CD3}$. We note the same set of DNA strands (Figure 2a) can be used to generate a tetraspecific antibody that targets the tumor cells more specifically by having, for example, two scFvs that bind to two different tumor surface antigens. Even in the current study, having two anti-CD19 scFvs should theoretically achieve greater specificity for $CD19^+$ cells via avidity effect. Higher order specificity is gaining interest even in therapeutic area outside of immunotherapy. For example, studies have shown that trispecific antibodies targeting three different, highly conserved epitopes of the HIV-1 envelope protein can achieve greater neutralization breadth and potency than single broadly neutralizing antibodies.[28,29]

Finally, the NAPPA method is, of course, not limited to assembling scFvs. While the assembly modules are nucleic acids, the antigen binding modules can be scFv, nanobody, Fab, or combination of the three. Nanobody, Fab, and scFv are generally less stable than IgG, but afford the option of high level expression in bacteria,[30–32] which is cultured in inexpensive media.

4. Conclusion

In conclusion, the NAPPA method represents an entirely different means of generating MsAbs. Although the pharmacokinetics and potential toxicity of antibody-nucleic acid conjugates remain to be rigorously tested in higher animals, our current data suggest that the MsAbs assembled by NAPPA can engage T-cells and tumor cells similar to the well-known BsAbs. Therefore, with further optimization, the NAPPA method could potentially be a general solution for generating antibodies with higher order specificity, e.g., trispecific, tetraspecific, or higher. Given the ever growing database of effective cancer-specific antigens for immunotherapy, the versatile NAPPA approach potentially also allows rather convenient construction of a library of MsAbs for personalized cancer immunotherapy.

5. Experimental Section

The Experimental Section is available in the Supporting Information. All animal experiments were done according to the American Animal Protection Law with permission from the responsible local authorities.

Supporting Information

Supporting Information is available from the Wiley Online Library or from the author.

Acknowledgements

L.P. and C.C. contributed equally to this work. This study was supported by internal research fund from the Assembly Medicine, LLC.

Conflict of Interest

L.P. and J.J.C. are on the scientific advisory board of Assembly Medicine, LLC. C.C., L.P., and J.J.C. have ownership interests in Assembly Medicine, LLC. No potential conflicts of interest were disclosed by other authors.

Keywords

antibody library, immunotherapy, multispecific antibodies, self-assembly, T-cell engaging

Received: April 29, 2019
Revised: October 22, 2019
Published online: November 23, 2019

[1] U. Brinkmann, R. E. Kontermann, *mAbs* **2017**, *9*, 182.
[2] A. F. Labrijn, M. L. Janmaat, J. M. Reichert, P. W. H. I. Parren, *Nature Reviews Drug Discovery* **2019**, *18*, 585.
[3] F. H. Valone, P. A. Kaufman, P. M. Guyre, L. D. Lewis, V. Memoli, Y. Deo, R. Graziano, J. L. Fisher, L. Meyer, M. Mrozek-Orlowski, *J. Clin. Oncol.* **1995**, *13*, 2281.
[4] A. Thakur, L. G. Lum, *Curr. Opin. Mol. Ther.* **2010**, *12*, 340.
[5] N. D. James, P. J. Atherton, J. Jones, A. J. Howie, S. Tchekmedyian, R. T. Curnow, *Br. J. Cancer* **2001**, *85*, 152.
[6] M. G. Fury, A. Lipton, K. M. Smith, C. B. Winston, D. G. Pfister, *Cancer Immunol. Immunother.* **2007**, *57*, 155.
[7] T. Nitta, K. Sato, H. Yagita, K. Okumura, S. Ishii, *Lancet* **1990**, *335*, 368.
[8] W. D. Mallender, E. W. Voss Jr., *J. Biol. Chem.* **1994**, *269*, 199.
[9] D. Saerens, G. H. Ghassabeh, S. Muyldermans, *Curr. Opin. Pharmacol.* **2008**, *8*, 600.
[10] D. Nagorsen, P. Kufer, P. A. Baeuerle, R. Bargou, *Pharmacol. Ther.* **2012**, *136*, 334.
[11] E. Wolf, R. Hofmeister, P. Kufer, B. Schlereth, P. A. Baeuerle, *Drug Discovery Today* **2005**, *10*, 1237.
[12] J. B. Ridgway, L. G. Presta, P. Carter, *Protein Eng., Des. Sel.* **1996**, *9*, 617.
[13] T. S. Von Kreudenstein, E. Escobar-Carbrera, P. I. Lario, I. D'Angelo, K. Brault, J. Kelly, Y. Durocher, J. Baardsnes, R. J. Woods, M. H. Xie, P. A. Girod, M. D. Suits, M. J. Boulanger, D. K. Poon, G. Y. Ng, S. B. Dixit, *mAbs* **2013**, *5*, 646.
[14] K. Gunasekaran, M. Pentony, M. Shen, L. Garrett, C. Forte, A. Woodward, S. B. Ng, T. Born, M. Retter, K. Manchulenko, H. Sweet, I. N. Foltz, M. Wittekind, W. Yan, *J. Biol. Chem.* **2010**, *285*, 19637.
[15] M. Bacac, T. Fauti, J. Sam, S. Colombetti, T. Weinzierl, D. Ouaret, W. Bodmer, S. Lehmann, T. Hofer, R. J. Hosse, E. Moessner, O. Ast, P. Bruenker, S. Grau-Richards, T. Schaller, A. Seidl, C. Gerdes, M. Perro, V. Nicolini, N. Steinhoff, S. Dudal, S. Neumann, T. von H irschheydt, C. Jaeger, J. Saro, V. Karanikas, C. Klein, P. Umana, *Clin. Cancer Res.* **2016**, *22*, 3286.
[16] J. J. Chou, L. Pan, *PCT/CN2018/080058*, **2017**.
[17] S. A. Kazane, J. Y. Axup, C. H. Kim, M. Ciobanu, E. D. Wold, S. Barluenga, B. A. Hutchins, P. G. Schultz, N. Winssinger, V. V. Smider, *J. Am. Chem. Soc.* **2013**, *135*, 340.

[18] M. P. Coyle, Q. Xu, S. Chiang, M. B. Francis, J. T. Groves, *J. Am. Chem. Soc.* **2013**, *135*, 5012.
[19] K. P. Williams, X. H. Liu, T. N. Schumacher, H. Y. Lin, D. A. Ausiello, P. S. Kim, D. P. Bartel, *Proc. Natl. Acad. Sci. USA* **1997**, *94*, 11285.
[20] M. J. Damha, P. A. Giannaris, P. Marfey, *Biochemistry* **1994**, *33*, 7877.
[21] M. Boyce, S. Warrington, B. Cortezi, S. Zollner, S. Vauleon, D. W. Swinkels, L. Summo, F. Schwoebel, K. Riecke, *Br. J. Pharmacol.* **2016**, *173*, 1580.
[22] J. P. Van Wauwe, J. R. De Mey, J. G. Goossens, *J. Immunol.* **1980**, *124*, 2708.
[23] J. Wang, S. Tian, R. A. Petros, M. E. Napier, J. M. Desimone, *J. Am. Chem. Soc.* **2010**, *132*, 11306.
[24] H. Durbin, S. Young, L. M. Stewart, F. Wrba, A. J. Rowan, D. Snary, W. F. Bodmer, *Proc. Natl. Acad. Sci. USA* **1994**, *91*, 4313.
[25] R. B. Greenwald, Y. H. Choe, J. McGuire, C. D. Conover, *Adv. Drug Delivery Rev.* **2003**, *55*, 217.
[26] N. Jain, S. W. Smith, S. Ghone, B. Tomczuk, *Pharm. Res.* **2015**, *32*, 3526.
[27] S. Girish, M. Gupta, B. Wang, D. Lu, I. E. Krop, C. L. Vogel, H. A. Burris Iii, P. M. LoRusso, J. H. Yi, O. Saad, B. Tong, Y. W. Chu, S. Holden, A. Joshi, *Cancer Chemother. Pharmacol.* **2012**, *69*, 1229.
[28] L. Xu, A. Pegu, E. Rao, N. Doria-Rose, J. Beninga, K. McKee, D. M. Lord, R. R. Wei, G. Deng, M. Louder, S. D. Schmidt, Z. Mankoff, L. Wu, M. Asokan, C. Beil, C. Lange, W. D. Leuschner, J. Kruip, R. Sendak, Y. D. Kwon, T. Zhou, X. Chen, R. T. Bailer, K. Wang, M. Choe, L. J. Tartaglia, D. H. Barouch, S. O'Dell, J. P. Todd, D. R. Burton, M. Roederer, M. Connors, R. A. Koup, P. D. Kwong, Z. Y. Yang, J. R. Mascola, G. J. Nabel, *Science* **2017**, *358*, 85.
[29] J. J. Steinhardt, J. Guenaga, H. L. Turner, K. McKee, M. K. Louder, S. O'Dell, C. I. Chiang, L. Lei, A. Galkin, A. K. Andrianov, A. D.-R. N, R. T. Bailer, A. B. Ward, J. R. Mascola, Y. Li, *Nat. Commun.* **2018**, *9*, 877.
[30] E. Pardon, T. Laeremans, S. Triest, S. G. Rasmussen, A. Wohlkonig, A. Ruf, S. Muyldermans, W. G. Hol, B. K. Kobilka, J. Steyaert, *Nat. Protoc.* **2014**, *9*, 674.
[31] P. Carter, R. F. Kelley, M. L. Rodrigues, B. Snedecor, M. Covarrubias, M. D. Velligan, W. L. Wong, A. M. Rowland, C. E. Kotts, M. E. Carver, M. Yang, J. H. Bourell, H. M. Shepard, D. Henner, *Biotechnology* **1992**, *10*, 163.
[32] K. D. Miller, J. Weaver-Feldhaus, S. A. Gray, R. W. Siegel, M. J. Feldhaus, *Protein Expression Purif.* **2005**, *42*, 255.

ADVANCED SCIENCE
Open Access

Supporting Information

for *Adv. Sci.*, DOI: 10.1002/advs.201900973

DNA-Mediated Assembly of Multispecific Antibodies for T Cell Engaging and Tumor Killing

*Liqiang Pan, Chan Cao, Changqing Run, Liujuan Zhou, and James J. Chou**

Supporting Information

DNA-mediated assembly of multi-specific antibodies for T cell engaging and tumor killing

Liqiang Pan, Chan Cao, Changqing Run, Liujuan Zhou, and James J. Chou

Methods

L-DNA preparation

L-DNA amidites (Beta-L-deoxy Adenosine (n-bz) CED phosphoramidite, Beta-L-deoxy Guanosine (n-ibu) CED phosphoramidite, Beta-L-Thymidine CED phosphoramidite and Beta-L-deoxy Cytidine (n-acetyl) CED phosphoramidite) were synthesized by ChemGenes (Massachusetts, USA). Four 5'-modified (NH_2-C6) L-DNA fragments (designed to form Holliday junction) were synthesized and purified by Bio-Synthesis (Texas, USA). The four L-DNA fragments are:

L-DNA1 (5'-AAGAGGACGCAATCCTGAGCACGAGGTCT-3'),

L-DNA2 (5'-AACTGCTGCCATAGTGGATTGCGTCCTCT-3'),

L-DNA3 (5'-AATGAGTGCATTCGGACTATCCGAGCAGT-3'), and

L-DNA4 (5'-AAGACCTCGTGCTCACCGAATGCACTCAT-3').

L-DNA assembly and stability

To test L-DNA assembly, L-DNAs were mixed at equal molar ratio (10 μM each) at room temperature for 1 min, followed by examination with 3% agarose gel. For evaluating the resistance of the L-DNAs to nucleases, four corresponding D-DNAs (with identical sequence to L-DNA) were synthesized and assembled. Assembled L-DNA and D-DNA tetramers were treated at 37 °C for 24 h with different

nucleases, including DNase I (Thermo Scientific, AM2222), Exonuclease I (NEB, M0293S), S1 Nuclease (Thermo Scientific, EN0321), and T7 Endonuclease I (NEB, M0302S). The D/L-DNA samples treated with nucleases were examined with 3% agarose gel. To test L-DNA tetramer stability in serum, L-DNA tetramer was mixed with Fetal bovine serum (Gibco) at equal volume ratio (1:1), followed by incubation at 37 °C for 1 h, 4 h, 24 h or 48 h. Samples were examined with 2% agarose gel electrophoresis.

scFv expression and purification

Gene fragment encoding H6-MBP-(TEV site)-Strep-scFv were subcloned into the pET21(+) vector (Novagen) to generate scFv expression plasmids. Expression constructs were transformed into SHuffle T7 competent *E.coli* cells (New England Biolabs). The cells were grown at 37 ℃ in LB media until the OD600 reached 0.6~0.8. Then the cell culture was cooled to 16 ℃ before adding 0.1 mM β-D-thiogalatopyranoside (IPTG), and protein expression lasted overnight at 16 ℃. The cells were harvested and resuspended in lysis buffer (20 mM Tris-HCl, 200 mM NaCl, 2 mM EDTA, 10 μM TCEP, pH 7.4), followed by sonication with a 6 mm probe (20% output) for 5 min. The cell lysis was centrifuged at 40,000 g for 25 min at 4 ℃ and the supernatant was loaded to an amylose column (New England Biolabs) pre-equilibrated with the lysis buffer. The fusion protein was eluted with 4 column volumn (CV) of lysis buffer supplemented with 10 mM D-maltose (Sigma). The purified fusion protein was cleaved with tobacco etch virus (TEV) protease (at a concentration of 10 μg/ml) for 2 h at 37 ℃ to remove the MBP, followed by further purification by size exclusion chromatography (Superdex 200 Increase, GE lifescience). The elution fractions containing the Strep-tagged scFv were collected and stored at -80 ℃.

SPR measurement of scFv affinity to target antigens

SPR measurements were performed using the Biacore 8K instrument (GE Life Sciences) at 25 °C. Human CD19 ($CD19_{20-291}$-10xHis, Acro Biosystems, Cat# CD9-H52H2) or CD3 ($CD3_{23-126}$-6xHis, Abcam, Cat# ab220577) antigen proteins were coupled to the CM5 chip surface by amino coupling. To measure binding, purified MBP-scFvs in the SPR buffer was injected at increasing concentrations (0.0078125, 0.015625, 0.03125, 0.0625, 0.125, 0.25 and 0.5 μM). The response in signal (RU) at each of the above protein concentration was recorded (**Figure S1**). SPR data processing and analysis were performed using the program BIAevaluation (GE Life Sciences). Equilibrium signal (R_{eq}) at different MBP-scFv concentration (C) were plotted and fit to the equation $R_{eq} = R_{max}/(1 + K_D/C)$ to determine the equilibrium binding constant (K_D). R_{max} is the binding signal at saturation.

scFv-DNA ligation

The L-DNA with a 5'-NH_2 group was dissolved in PBS (10 mM Na_2HPO_4, 1.8 mM KH_2PO_4, 2.7 mM KCl, 137 mM NaCl, pH7.4) to a concentration of 0.5 mM. In order to ligate scFv with L-DNA, a mixture of

L-DNA and SM(PEG)$_2$ (ThermoFisher) at a molar ratio of 1 : 50 was first incubated at 25 ℃ for 2 h to ligate SM(PEG)$_2$ with L-DNA. Precipitate formed immediately after adding 2 volumns of anhydrous ethanol. Following incubation at -20 ℃ for 20 min, the precipitate was collected by centrifuging at 12000 rpm for 10 min and the supernatant was removed. The pellet was washed with 75% ethanol for 4 times. The residual ethanol was vaporized and the pellet was solubilized with double distilled water to a concentration of ~ 5 mg/ml. The SM(PEG)$_2$-DNA was stored at -80 ℃.

ScFv was mixed with SM(PEG)$_2$-DNA at a molar ratio of 1:1.2 - 1:2 at 4 ℃ for overnight to ligate scFv with L-DNA. The conjugation yield was ~90%. Unligated SM(PEG)$_2$-DNA was removed by passing through a strepTactin (Qiagen) column (**Figure S6a**). The elution was further loaded on a HiTrap Q column (GE lifescience) and scFv-DNA was eluted by a 20 CV linear gradient from buffer A (20 mM Tris-HCl, 15 mM NaCl, pH 8.5) to buffer B (20 mM Tris-HCl, 1 M NaCl, pH 8.5). The elution fractions containing scFv-DNA was collected and dialysis against PBS for 1.5 h for twice (**Figure S6b**). The sample was concentrated to a concentration of 10 μM.

Protein assembly

The tri-specific antibody with two anti-CD19 units and an anti-CD3 unit were prepared by mixing an equal amount of anti-CD19-HJ1, anti-CD19-HJ2, free HJ3 and anti-CD3-HJ4. The quad-specific antibody with two anti-CD19 units and two anti-CD3 unit were prepared by mixing an equal amount of anti-CD19-HJ1, anti-CD19-HJ2, anti-CD3-HJ3 and anti-CD3-HJ4. The quad-specific antibody with two anti-CD19 units, an anti-41BB units and an anti-CD3 unit were prepared by mixing an equal amount of anti-CD19-HJ1, anti-CD19-HJ2, anti-41BB-HJ3 and anti-CD3-HJ4. All the assemblies were stored at -80 ℃.

Cell cultures

Human Burkitt's lymphoma Raji cell line. Raji cells were cultured in RPMI medium (Gibco, ThermoFisher Scientific) supplemented with 10% Fetal Bovine Serum (Gibco, ThermoFisher Scientific) and 100 U/ml Pen-Strep (GIBCO, ThermoFisher Scientific), in a 37 °C, 5% CO_2 incubator (ThermoFisher Scientific).

Human colorectal adenocarcinoma LS174T cell line. LS174T cells were maintained in EMEM medium (Gibco, ThermoFisher Scientific) supplemented with 10% Fetal Bovine Serum and 100 U/ml Pen-Strep (GIBCO, ThermoFisher Scientific), in a 37 °C, 5% CO_2 incubator (ThermoFisher Scientific).

Human peripheral blood mononuclear cells (PBMC). For *in vitro* efficacy study, PBMCs were separated from the whole blood of healthy donors by a density gradient centrifugation method using

Ficoll Histopaque. For *in vivo* studies, PBMCs were purchased from appropriate vendors (ASTARTE BIOLOGICS).

In vitro cytotoxicity of NAPPA001 and NAPPA002

In each of the 96-well plates, Raji cells (10^4) were mixed with fresh human PBMCs (10^5) at E:T ratio of 10:1, followed by the addition of various concentrations of $(scFv^{CD19})_2$-$scFv^{CD3}$ (NAPPA001). Raji cell lysis was assessed after 48 hours of MsAb treatment using a LDH detection kit (Beyotime, China). LDH stands for lactate dehydrogenase; it is released into the extracellular media by dead cells due to impaired membrane integrity. Cytotoxicity (%) was calculated as [sample LDH release – background LDH release]/[maximum LDH release – background LDH release] × 100, where background LDH release is from Raji cells incubated with PBMC without MsAbs and maximum LDH release is from Raji cells treated with 1% Triton X-100. All measurements were performed in triplicates. The same protocol was used for other positive and negative control experiments. Exactly the same protocol was also used for measuring *in vitro* cytotoxicity of $(scFv^{CEA})_2$-$scFv^{CD3}$ (NAPPA002) on the LS174T colon carcinoma cells.

T-cell activation by $(scFv^{CD19})_2$-$scFv^{CD3}$ (NAPPA001)

Raji cells were seeded in 96-well plate at a density of 10,000 cells/well, and mixed with fresh human PBMCs at E:T ratio of 10:1. $(scFv^{CD19})_2$-$scFv^{CD3}$ After 48 hours treatment with $(scFv^{CD19})_2$-$scFv^{CD3}$ at different concentrations (0.1 pM, 10 pM, 1 nM), cells from each well were divided into two aliquots for measuring cell surface expression of CD25 and CD137, respectively.

For CD25 immunostaining, cells from one aliquot were incubated with Rabbit anti-human CD3ε mAb (1/1000 dilution, Abcam, Cat# ab52959) for 30 min and with Mouse anti-human CD25 mAb (0.5 μg/test, Thermo Fisher scientific, Cat# MA5-12680) for 60 min on ice. After washing, cells were further incubated with Goat anti-Mouse IgG H&L (Alexa Fluor 488) (1/2000 dilution, Abcam, Cat# ab150113) and Donkey anti-Rabbit IgG H&L (Alexa Fluor 647) (1/2000 dilution, Abcam, Cat# ab150075) for 30 min on ice. After washing, the cells were examined by flow cytometry, and $CD3^+$ cells were gated for further evaluation of CD25 expression level.

For CD137 (also known as 4-1BB) immunostaining, cells from the other aliquot were incubated with Rabbit anti-human CD137 mAb (1/400 dilution, Cell Signaling Technology, Cat# 34594) for 1 hour on ice. After washing, cells were further incubated with Mouse anti-human CD3ε mAb [UCHT1] (1/100 dilution, Abcam, Cat# ab34275) and Donkey anti-Rabbit IgG H&L (Alexa Fluor 647) (1/2000 dilution, Abcam, Cat# ab150075) for 30 min on ice. After washing, cells were examined by flow cytometry, and $CD3^+$ cells were gated for further evaluation of CD137 expression level.

Animal study

Mice. Female (non-pregnant and nulliparous) NOD-*scid* IL2Rgamma^{null} (The Jackson

Laboratory, Lot# 005557) mice (age 6-8 weeks) were used for human carcinoma xenograft mouse model. Mice were maintained under pathogen-free and standardized environmental conditions (20±1 °C, 50±10% relative humidity, 12 hours light-dark daily cycles). All experiments were done according to the American Animal Protection Law with permission from the responsible local authorities.

In vivo efficacy of $(scFv^{CD19})_2$-$scFv^{CD3}$ (NAPPA001). Raji cells (5×10^5 cells) (50 μL) were pre-mixed with human PBMC (2×10^6 cells) (50 μL) at an E:T ratio of 4:1, and further mixed with Matrigel (100 μL) in a 1:1 ratio yielding 200 μL suspension for subcutaneous implantation into the right flanks of NOD/SCID mice. The $(scFv^{CD19})_2$-$scFv^{CD3}$ (0.5 mg per 1 kg of body mass) was injected intravenously twice a week for four weeks starting 3 days after Raji/PBMC co-grafting. Caliper tumor volume measurements were made twice-weekly on all surviving animals. Tumor volumes were estimated by the following formula: Tumor Volume = 0.5 × (length × width^2), where length is the longest diameter measurement and width is the shortest diameter measurement.

In vivo efficacy of $(scFv^{CEA})_2$-$scFv^{CD3}$ (NAPPA002). LS174T cells (10^6) were pre-mixed with PBMCs (5×10^6) at an E:T ratio of 5:1, and further mixed with Matrigel in a 1:1 ratio yielding 200 μL suspension for subcutaneous implantation into the right flanks of NOD/SCID mice. The $(scFv^{CEA})_2$-$scFv^{CD3}$ (1 mg per 1 kg of body mass) was injected intravenously twice a week for 1.5 weeks starting 3 days after LS174T/PBMC co-grafting. Caliper tumor volume measurements were made twice-weekly on all surviving animals. Tumor volumes were estimated by the following formula: Tumor Volume = 0.5 × (length × width^2), where length is the longest diameter measurement and width is the shortest diameter measurement.

In vivo imaging of MsAbs targeting solid tumor. LS174T cells (10^6) were pre-mixed with PBMCs (5×10^6) at an E:T ratio of 5:1, and further mixed with Matrigel in a 1:1 ratio yielding 200 μL suspension for subcutaneous implantation into the right flanks of NOD/SCID mice. When tumor volume reached ~500 mm^3, $(scFv^{CEA})_2$-$scFv^{CD3}$-Cy5.5 (220 μL, 0.45 mg/ml) or PBS (vehicle) was injected intravenously. Fluorescence intensity in mice was recorded and quantified by a small animal imager (PerkinElmer IVIS Kinetic III) at different time points (1, 2, 4, 8, 24, 48, 96 h). Fluorescence intensity vs. Time curve was generated to determine half-life of the fluorescent MsAb in mice.

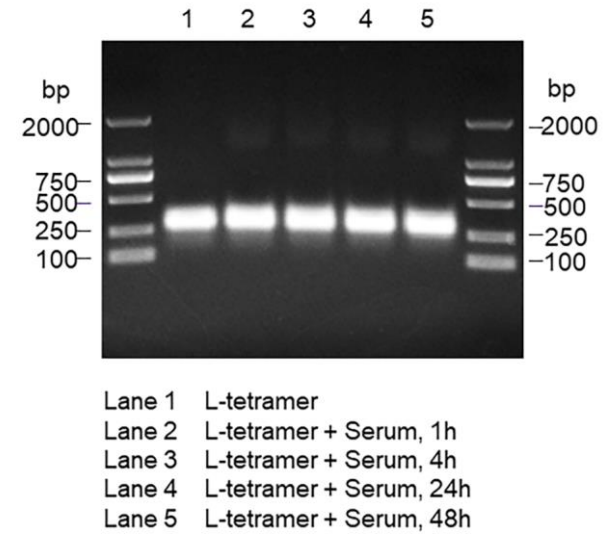

Figure S1. Stability of L-DNA tetramer in serum.

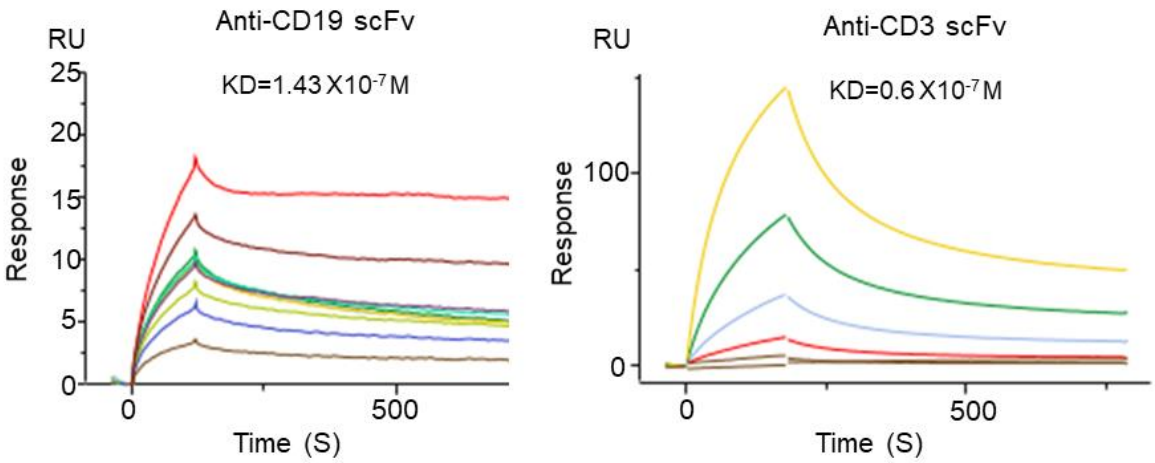

Figure S2. Determination of scFv affinity by Surface Plasmon Resonance (SPR).

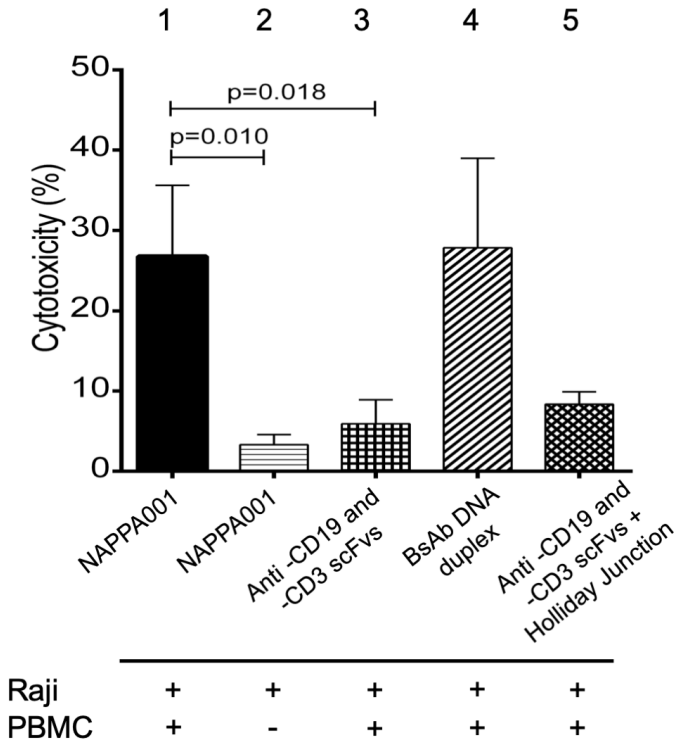

Figure S3. Negative and positive controls for T-cell redirected killing of Raji cells mediated by NAPPA001. To examine whether cancer cell killing was due to T-cell redirecting, Raji cells were treated with 500 pM NAPPA001 in the presence (**1**) or absence (**2**) of hPBMC (E:T=10:1) for 2 days. To examine whether the cancer cell killing on the left was due to T-cell – Raji engaging mediated by the bispecific NAPPA001, Raji cells were treated with a mixture of $scFv^{CD19}$ and $scFv^{CD3}$ (500 pM) in the presence of hPBMC (E:T=10:1) (**3**). To test whether $scFv^{CD19}$-$scFv^{CD3}$ assembled with a simple L-DNA duplex can function as a normal BsAb, $scFv^{CD19}$-L-DNA1 and $scFv^{CD3}$-L-DNA4 were mixed at 1:1 ratio. Raji cells were treated with 500 pM of BsAb in the presence of hPBMC (E:T=10:1) for 2 days (**4**). To ensure that antibody assembly was mediated by L-DNA oligomerization, the $scFv^{CD19}$ and $scFv^{CD3}$ were mixed with L-DNA Holliday junction at 500 pM each and used to treat Raji cells in the presence of hPBMC (E:T=10:1) (**5**). Tumor lysis (cytotoxicity) was measured using the LDH (lactate dehydrogenase) detection kit, which quantifies LDH release from dead cells with impaired membrane integrity.

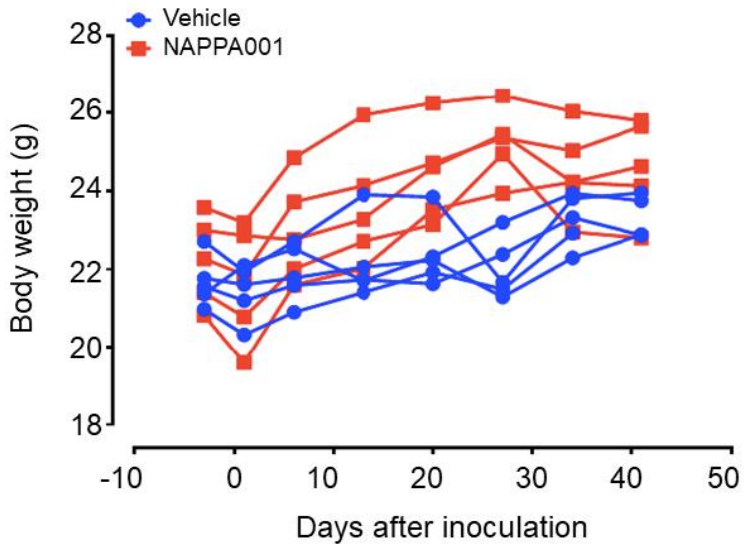

Figure S4. Body weights of the five mice during *in vivo* efficacy study of $(scFv^{CD19})_2$-$scFv^{CD3}$ (NAPPA001).

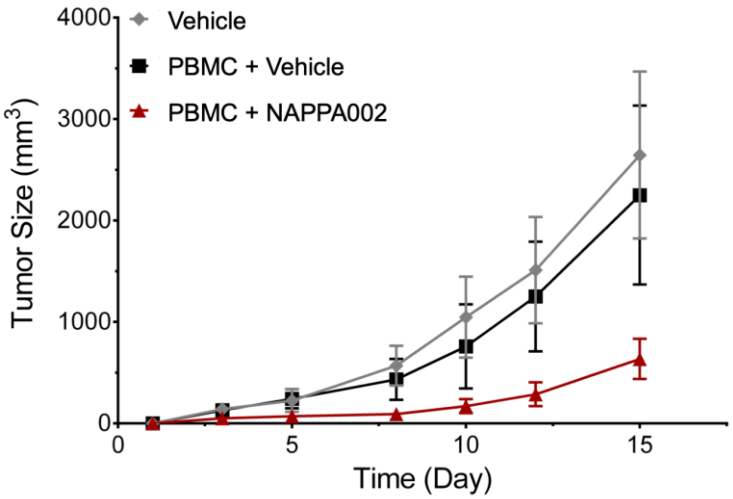

Figure S5. *In vivo* efficacy of NAPPA002 in human colorectal adenocarcinoma (LS174T cell line) xenograft mouse model. LS174T tumor cells were implanted or co-implanted with human PBMC (E:T ratio is 5:1) subcutaneously into NSG mice (n = 6) and treated with either

PBS (vehicle) in the absence (gray) or presence (black) of PBMC, or NAPPA002 (20 μg/mouse) (red) via intravenous injection twice a week starting 3 days after LS174T/PBMC co-grafting for 1.5 weeks.

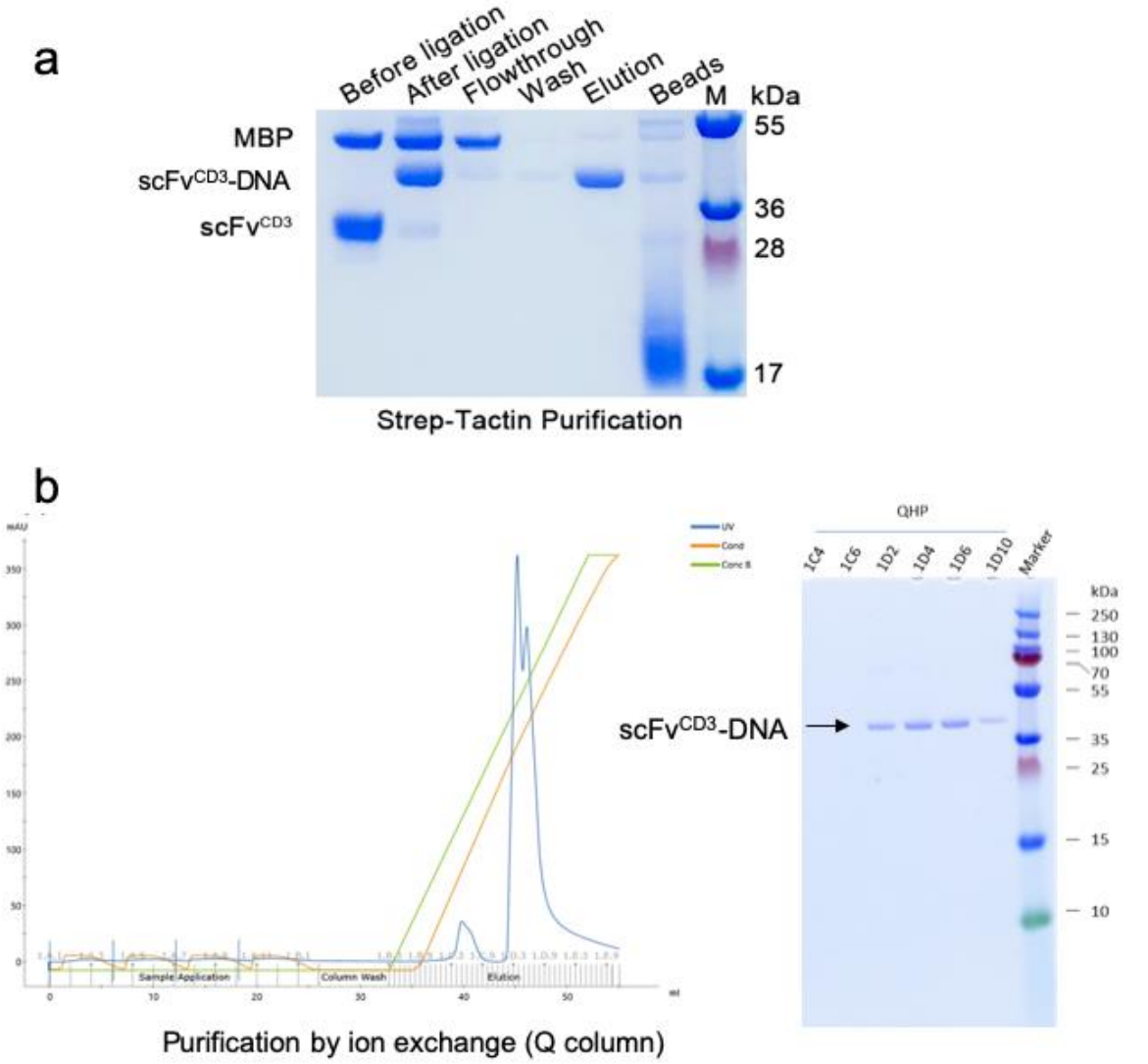

Figure S6. Preparation and purification of scFv-DNA. The scFv released from the MBP fusion protein was mixed with $SM(PEG)_2$-L-DNA at a molar ratio of 1:1.2 - 1:2 at 4 ℃ for overnight to ligate scFv with L-DNA. (**a**) SDS-PAGE analysis of scFv-DNA ligation and removal of unligated DNA by passing through a strepTactin (Qiagen) column. The conjugation yield was ~90%. (**b**) Ion exchange purification of the sample from (a) to remove unligated protein. Elution fractions from the HiTrap Q column (GE lifescience) were analyzed by SDS-PAGE.